

Article

CuAAC-Based Assembly and Characterization of a New Molecular Dyad for Single Material Organic Solar Cell

Antoine Labrunie ¹, Teddy Lebailly ¹, Amir Hossein Habibi ¹, Clément Dalinot ¹, Yue Jiang ², Sylvie Dabos-Seignon ¹, Jean Roncali ^{1,3}, Philippe Blanchard ^{1,*} and Clément Cabanetos ^{1,*}

¹ UMR CNRS 6200, MOLTECH-Anjou, UNIV Angers, 2 Bd Lavoisier, 49045 Angers, France; antoine.labrunie@univ-angers.fr (A.L.); teddy.lebailly@gmail.com (T.L.); amirhossein.habibi@etud.univ-angers.fr (A.H.H.); clement.dalinot@univ-angers.fr (C.D.); sylvie.dabos@gmail.com (S.D.-S.); jeanroncali@gmail.com (J.R.)

² Institute for Advanced Materials, Academy of Advanced Optoelectronics, and Guangdong Provincial Key Laboratory of Quantum Engineering and Quantum Materials, South China Normal University, Guangzhou 510006, China; jiangyue871116@gmail.com

³ Supramolecular Organic and Organometallic Chemistry Center Babes-Bolyai University, 400028 Cluj-Napoca, Romania

* Correspondence: philippe.blanchard@univ-angers.fr (P.B.); clement.cabanetos@univ-angers.fr (C.C.)

Received: 9 May 2019; Accepted: 23 May 2019; Published: 28 May 2019



Abstract: The synthesis and characterization of a new molecular dyad consisting of a benzodithiophene-based push-pull linked to a fullerene derivative through the use of the well-known Copper Azide-Alkyne Huisgen Cycloaddition (CuAAC) reaction is reported herein. Once fully characterized at the molecular level, single component organic solar cells were fabricated to demonstrate photon-to-electron conversion, and therefore the design principle.

Keywords: organic photovoltaics; organic synthesis; molecular dyad; single-materials organic solar cells

1. Introduction

To cut back production costs, the development of organic photovoltaic (OPV) cells has attracted considerable research interest over the previous decades due to its advantages such as an easy scalable, versatile and low cost processing techniques as well as a potential compatibility with flexible substrates. Consequently, power conversion efficiency (PCE) has consistently grown, now exceeding 15% in bulk heterojunction organic solar cells [1]. With active layers based on a blend of an electron donor (D) and an electron acceptor (A), several empirical parameters must be routinely adjusted to reach such efficiencies, such as the D/A ratio, the nature of the processing solvent, different annealing conditions, and/or the use of additives [2–8]. Moreover, it is noteworthy that, even if an optimized morphology is luckily achieved, the latter usually evolves leading, in general, to a drastic decrease in the device performances [9–11].

One possible strategy to solve this problem relies in the use of a unique active material where a donor and an acceptor moiety would be connected through a covalent or eventually supramolecular bridge/binding [12,13]. Ideally, such a single ambipolar material would be able to absorb light, dissociate excitons and transport photo-induced charges to the electrodes [14]. The synthesis of such a compound would lead to single-materials organic solar cells (SMOSCs) characterized by a potential simplified fabrication and improved stability since the morphology of the active layer should be less subjected to phase segregation. Despite the obvious interest of this concept, only few molecular

materials have been evaluated in SMOSCs and even fewer reached PCEs above 0.5% [15–20] with a maximum reported at 2.2% and 2.4% for a C₆₀ based dyad and a triad respectively [21,22].

In this challenging context, our group has recently reported several synthetically accessible examples of molecular dyads consisting of arylamine based donor push–pulls linked to a fullerene (C₆₀) derivative via a triazole σ -linker (Figure 1) [20,23].

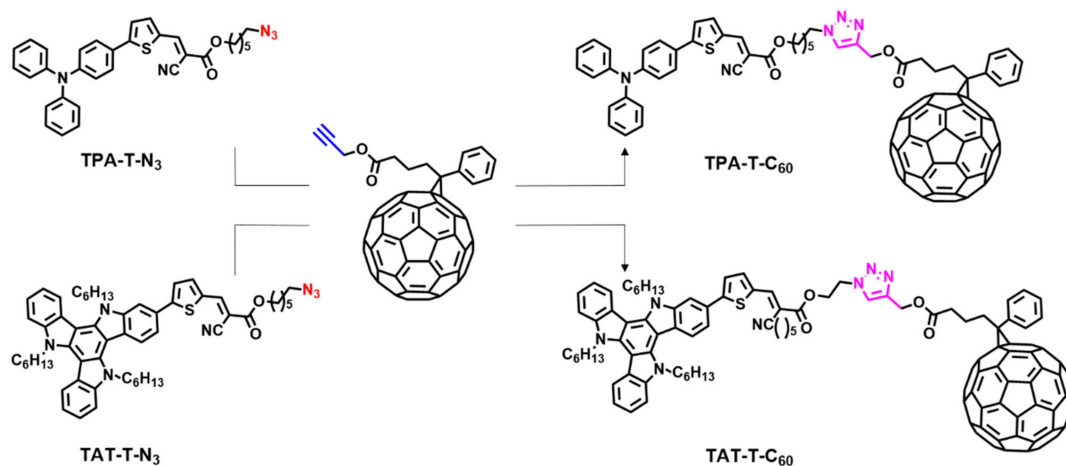


Figure 1. Illustration of our early reported molecular dyads and strategies.

Although modest efficiencies were achieved in both cases (0.4% and 0.6% for TPA-T-C₆₀ and TAT-T-C₆₀ respectively), these preliminary results demonstrated that (i) click chemistry is an efficient, versatile and easy strategy to build such D-A architectures and (ii) charge percolation within the respective active layers is somehow possible.

Motivated by this challenging topic, we report herein the synthesis and preliminary evaluation of a benzodithiophene based push-pull molecular donor clicked, via a Copper Azide-Alkyne Huisgen Cycloaddition (CuAAC) reaction, to a fullerene derivative as single material for OPV (Figure 2).

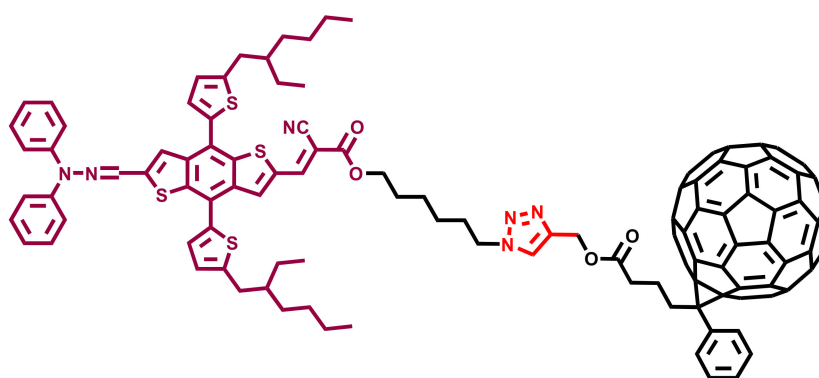


Figure 2. Illustration of the two molecules studied herein.

The well-known benzo[1,2-*b*:4,5-*b'*]dithiophene (BDT) unit was chosen as a central building block for its extended conjugation, planar structure and good hole transporting properties [24–27]. In addition, to expand the spectral absorption range of the molecular donor within a minimum of synthetic effort, the BDT core was dissymmetrized and functionalized at one extremity by an electron rich moiety (diphenyl hydrazine) and on the other one by an electron deficient block namely a cyano vinyl ester.

2. Materials and Methods

All reagents and chemicals from commercial sources were used without further purification. Solvents were dried and purified using standard techniques. Column chromatography was performed with analytical-grade solvents using Aldrich silica gel (technical grade, pore size 60 Å, 230–400 mesh particle size). Flexible plates ALUGRAM® Xtra SIL G UV254 (MACHEREY-NAGEL, Düren, Germany) were used for TLC. Compounds were detected by UV irradiation (Thermo Fisher Scientific, Waltham, MA, USA) or staining with diiodine, unless otherwise stated. NMR spectra were recorded with an AVANCE III 300 (Bruker, Billerica, MA, USA) (^1H , 300 MHz and ^{13}C , 75 MHz) and Bruker AVANCE DRX 500 (Bruker, Billerica, MA, USA) (^1H , 500 MHz and ^{13}C , 125 MHz). Chemical shifts are given in ppm relative to tetramethylsilane TMS and coupling constants J in Hz. Residual non-deuterated solvent was used as an internal standard. UV-Vis absorption spectra were recorded at room temperature on a Perkin Elmer Lambda 950 spectrometer or with a Shimadzu UV-1800. Matrix Assisted Laser Desorption/Ionization was performed on MALDI-TOF MS BIFLEX III Daltonics spectrometer (Bruker, Billerica, MA, USA) using dithranol, DCTB or α -terthiophene as matrix. Cyclic voltammetry was performed using a Biologic SP-150 potentiostat (Bio-Logic, Seyssinet-Pariset, France) with positive feedback compensation in dichloromethane solutions (HPLC grade, Thermo Fisher Scientific, Waltham, MA, USA). Tetrabutylammonium hexafluorophosphate (0.1 M as supporting electrolyte) was purchased from Sigma-Aldrich and recrystallized prior to use. Experiments were carried out under an inert atmosphere (Ar) using a glovebox, by scanning the negative potential first, in a one-compartment cell equipped with platinum working microelectrode ($\varnothing = 2$ mm) and a platinum wire counter electrode. A silver wire immersed in 0.10 M $\text{Bu}_4\text{NPF}_6/\text{CH}_2\text{Cl}_2$ was used as pseudo-reference electrode and checked against ferrocene/ferrocenium couple (Fc/Fc^+) before and after each experiment. Atomic force microscopy experiments were performed using the Nano-Observer device (CSI Instruments, Les Ulis, France). The topographic images were obtained at room temperature in tapping mode. Images were processed with the Gwyddion free SPM data analysis software (Gwyddion version 2.53, David Nečas and Petr Klapetek, Czech Republic).

Benzo[1-*b*:4,5-*b'*]dithiophene-4,8-dione (1) [26], 2-(2-ethylhexyl)thiophene (2) [25], 4,8-bis(5-(2-ethylhexyl)thiophen-2-yl)benzo[1,2-*b*:4,5-*b'*]dithiophene (3) [28], 4,8-bis(5-(2-ethylhexyl)thiophen-2-yl)benzo[1,2-*b*:4,5-*b'*]dithiophene-2,6-dicarbaldehyde (4), 6-bromohexyl 2-cyanoacetate (7) [23], 6-azidohexyl 2-cyanoacetate (8) [23], [6,6]-phenyl- C_{61} -butyric acid (PCBA) [23] and [6,6]-phenyl- C_{61} -butyric acid propargylic ester (9) [23] were synthesized according to previously reported methods.

6-((2,2-diphenylhydrazono)methyl)-4,8-bis(5-(2-ethylhexyl)thiophen-2-yl)benzo[1,2-*b*:4,5-*b'*]dithiophene-2-carbaldehyde (5): the bis aldehyde 4 (71.93 mg, 113.3 μmol) was first solubilized in 120 mL of dichloromethane. Sodium sulfate (32.2 mg, 226.5 μmol) was then added and the mixture was degassed by argon bubbling for 30 min before adding the crushed 2,2-diphenylhydrazine chloride (25 mg, 113.3 μmol , 1 equivalent). After a night of stirring at room temperature, volatile species were removed under vacuum and the resulting crude was purified via on silica gel using dichloromethane as eluent to afford the desired compound (70.1 mg, 77%). $^1\text{H NMR}$ (CDCl_3): $\delta = 10.03$ (1H, s), 8.30 (1H, s), 7.48–7.40 (4H, m), 7.37 (2H, d, $J = 4.7$ Hz), 7.32 (1H, s), 7.24–7.17 (7H, m), 6.98 (1H, d, $J = 3.5$ Hz), 6.84 (1H, d, $J = 3.5$ Hz), 2.92 (2H, d, $J = 6.8$ Hz) 2.82 (2H, d, $J = 6.7$ Hz), 1.81–1.69 (m, 1H), 1.68–1.59 (m, 1H), 1.57–1.22 (16H, m), 1.05–0.86 (12H, m). $^{13}\text{C NMR}$ (CDCl_3): $\delta = 184.79, 146.92, 146.46, 145.77, 143.16, 143.03, 141.57, 140.19, 139.19, 136.04, 135.99, 135.80, 134.85, 130.04, 130.0, 128.50, 128.19, 126.79, 125.93, 125.64, 125.32, 124.12, 122.64, 122.45, 41.67, 41.54, 34.50, 34.36, 32.68, 32.56, 29.08, 29.00, 25.96, 25.82, 23.17, 23.12, 14.32, 14.27, 11.12, 10.99$. HRMS (FAB): calculated for $\text{C}_{48}\text{H}_{52}\text{N}_2\text{O}_4$: 800.2962, found: 800.2963.

BDT-N₃: To a stirred solution of 5 (38 mg, 47.34 μmol) and the 6-azidohexyl-2-cyanoacetate 8 (19.9 mg, 94.9 μmol) in dichloromethane (15 mL) 2–3 drops of triethylamine were added. The reaction mixture was refluxed under argon for 3 days. Then the solvent was removed under vacuum and the residue was purified by column chromatography on silica gel (eluent: dichloromethane) affording

BDT-N₃ as a red solid (41 mg, 87%). ¹H NMR (CDCl₃): δ = 8.36 (1H, s), 8.22 (1H, s), 7.48–7.40 (4H, m), 7.37 (2H, d, J = 4.8 Hz), 7.32 (1H, s), 7.25–7.17 (7H, m), 6.98 (1H, d, J = 3.5 Hz), 6.85 (1H, d, J = 3.5 Hz), 4.3 (2H, t, J = 6.6 Hz), 3.29 (2H, t, J = 6.8 Hz), 2.92 (2H, d, J = 6.7 Hz), 2.82 (2H, d, J = 6.7 Hz), 1.82–1.70 (m 3H), 1.70–1.59 (3H, m), 1.52–1.24 (20H, m), 1.04–0.83 (12H, m). ¹³C NMR (CDCl₃): δ = 162.90, 147.68, 147.02, 146.56, 146.05, 143.00, 142.08, 140.42, 139.29, 136.81, 135.96, 135.93, 135.82, 135.26, 130.05, 129.98, 128.60, 128.22, 126.19, 125.95, 125.80, 125.36, 123.69, 122.64, 122.59, 115.40, 100.65, 66.52, 51.46, 41.66, 41.48, 34.50, 34.41, 32.67, 32.60, 29.06, 29.01, 28.87, 28.53, 26.47, 25.92, 25.83, 25.57, 23.17, 23.11, 14.32, 14.28, 11.10, 10.98. **HRMS** (FAB): calculated for C₅₇H₆₄N₆O₂S₄: 992.3974, found: 992.3979.

BDT-C₆₀: Five drops of *N,N,N',N'',N''*-pentamethyldiethylenetriamine (PMDETA) dispersed in HPLC grade toluene (50 mL) were degassed three times via the “freeze, pump and thaw” technique. This solution was transferred using a cannula into a Schlenk flask containing the fullerene derivative **9** (37.5 mg, 40.2 μmol), CuBr (0.27 mg, 1.9 μmol) and the **BDT-N₃** (38 mg, 38.2 μmol) under argon atmosphere. The reaction mixture was protected from light and stirred for one night. The solvent was then removed under vacuum and the residue was purified by chromatography on silica gel using a mixture of dichloromethane and ethyl acetate as eluent (from 100:0 *v/v* to 90:10 *v/v*). The resulting solid was further purified by dissolution in dichloromethane and subsequent precipitation with pentane to afford the pure expected **BDT C₆₀** (62 mg, 84%) as a brown reddish powder. ¹H NMR (CDCl₃): δ = 8.36 (1H, s), 8.22 (1H, s), 7.88 (2H, d, J = 7.0 Hz), 7.59 (1H, s), 7–7.40 (7H, m), 7.38–7.34 (1H + 1H, s + d, J = 3.5 Hz), 7.32 (1H, s), 7.24–7.16 (7H, m), 6.97 (1H, d, J = 3.5 Hz), 6.84 (1H, d, J = 3.5 Hz), 5.22 (2H, s), 4.35 (2H, t, J = 7.2 Hz), 4.29 (2H, t, J = 6.4 Hz), 2.94–2.79 (6H, m), 2.53 (2H, t, J = 7.4 Hz), 2.23–2.09 (2H, m), 2.01–1.87 (2H, m), 1.80–1.68 (2H, m), 1.53–1.24 (22H, m), 1.02–0.83 (12H, m). ¹³C NMR (CDCl₃) δ = 173.05, 162.88, 148.87, 147.85, 147.05, 146.57, 146.22, 145.90, 145.27, 145.24, 145.21, 145.13, 145.11, 144.86, 144.80, 144.76, 144.73, 144.58, 144.48, 144.10, 143.84, 143.80, 143.09, 143.07, 142.99, 142.92, 142.26, 142.20, 142.16, 141.06, 140.83, 140.52, 138.11, 137.66, 137.05, 136.83, 135.93, 135.91, 135.82, 135.26, 132.22, 130.06, 128.63, 128.57, 128.37, 128.22, 126.28, 125.98, 125.81, 125.37, 123.75, 122.66, 115.48, 100.46, 79.94, 66.39, 57.97, 51.91, 50.33, 41.64, 41.47, 34.51, 34.41, 34.01, 33.74, 32.67, 32.59, 30.22, 29.07, 29.01, 28.36, 26.14, 25.92, 25.83, 25.46, 23.18, 23.12, 22.36, 14.36, 14.31, 11.12, 11.01. **HRMS** (FAB): calculated for C₁₃₁H₇₈N₆O₄S₄: 1926.4976, found: 1926.5003.

2.1. Device Fabrication and Testing

Pre-patterned indium-tin oxide coated glass slides of 24 × 25 × 1.1 mm³ with a sheet resistance of RS = 7 Ω/sq were purchased from Visiontek Systems. The substrates were washed by successive ultrasonic baths, namely diluted Deconex[®] 12 PA-x solution (2% in water), acetone and isopropanol for 15 min each. Once dried under a stream of air, a UV-ozone plasma treatment (Ossila UV/Ozone cleaner E511) was performed for 15 min. A filtered aqueous solution of poly(3,4-ethylenedioxy-thiophene)-poly(styrenesulfonate) (PEDOT:PSS; Ossila AI 4083) through a 0.45 μm RC membrane (Minisart[®] RC 15) was spun-cast onto the ITO surface at 5000 rpm for 40 s before being baked at 120 °C for 30 min. The dyad **BDT-C₆₀** was then spun cast and devices were completed by the thermal deposition of aluminum (100 nm) at a pressure of 1.5 × 10⁻⁵ Torr through a shadow mask defining six cells of 27 mm² each (13.5 mm × 2 mm). J-V curves were recorded in the dark and under illumination using a Keithley 236 source-measure unit and a home-made acquisition program. The light source used was an AM1.5 Oriel Solar sol3A Class AAA (Newport, MKS Instruments, Inc, Andover, MA, USA). The light intensity was measured by a broad-band power meter (13PEM001, Melles Griot). EQE were performed under ambient atmosphere using a halogen lamp (Osram) with an Action Spectra Pro 150 monochromator (Teledyne Technologies Inc, Thousand Oaks, USA) a lock-in amplifier (Perkin-Elmer 7225, Waltham, MA, USA) and a S2281 photodiode (Hamamatsu, Bridgewater Township, NJ, USA).

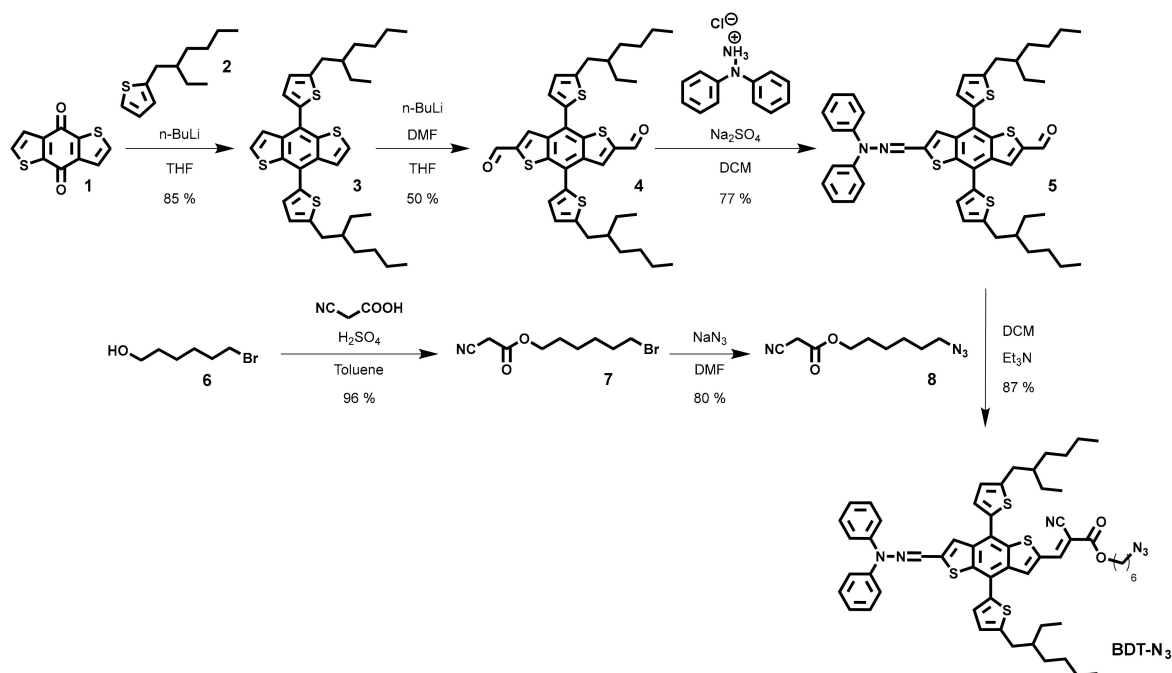
2.2. Space Charge Limited Current (SCLC) Measurements

The dyad was solubilized in chloroform at a concentration of 20 mg/mL, stirred at room temperature for 30 min, filtered through a 0.45 μm PTFE membrane and spun cast at 1000 rpm on the above

described PEDOT: PSS substrates to provide organic layers of *ca* 180 nm. Gold cathodes (150 nm) were thermally evaporated under a vacuum of 1.5×10^{-5} Torr, through a shadow mask defining active area of 12.60 mm², 3.10 mm² and 0.78 mm² per substrates. Hole mobilities μ^h were evaluated using the Mott-Gurney law, i.e., $J_{SCLC} = (9/8)\epsilon_0\epsilon_r\mu^h(V^2/d^3)$ where ϵ_r is the static dielectric constant of the medium ($\epsilon_r = 3$) and *d*, the thickness of the active layer, estimated at *ca* 180 nm through the use of an Alpha-Step Tencor D-500 profilometer [29].

3. Results and Discussion

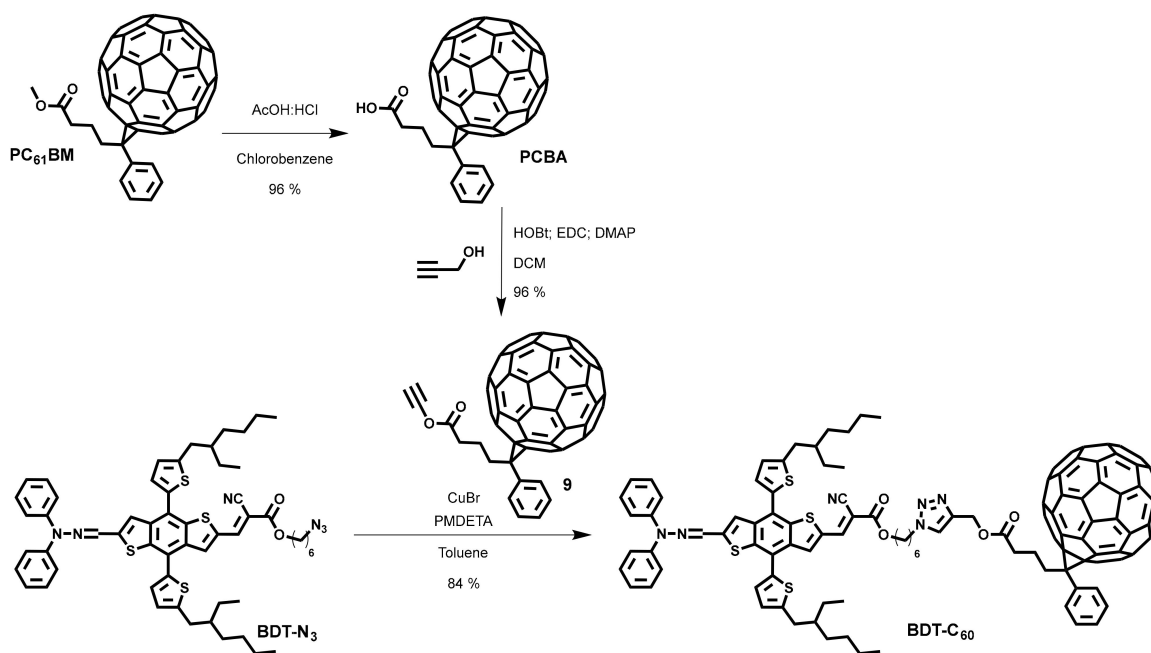
The synthetic route to the azido derivative **BDT-N₃** is depicted in Scheme 1.



Scheme 1. Synthetic route to **BDT-N₃**.

The thiophene-substituted benzodithiophene **3** was first prepared by addition of the lithiated 2-(2-ethylhexyl)thiophene **2** on commercially available thieno[2,3-*f*]benzothiophene-4,8-dione **1**.²⁸ The aldehyde moieties were then installed by the successive deprotonation and quenching of the lithiated intermediate with dry *N,N*-dimethylformamide (DMF). Thereafter, the resulting compound (**4**) was engaged in a reaction with only one equivalent of *N,N*-diphenylhydrazine in diluted media yielding the mono hydrazone based aldehyde **5** [30].

The σ -connector **8** was prepared in parallel by esterification of the 2-cyanoacetic acid in presence of 6-bromohexan-1-ol **6** followed by a nucleophilic substitution of the bromine by sodium azide.²³ The latter was then engaged in a Knoevenagel condensation with the aldehyde **5** thus affording the azido functionalized push-pull moiety **BDT-N₃**. The complementary reactive function, namely the alkyne, was introduced on the fullerene derivative via a subsequent saponification in acidic conditions of the commercially available **PC₆₁BM** followed by an esterification of the resulting [6,6]-Phenyl C₆₁ butyric acid (**PCBA**) intermediate with the propargyl alcohol (Scheme 2).



Scheme 2. Preparation of the molecular dyad **BDT-C₆₀**.

The later was finally clicked with the azido functionalized derivative **BDT-N₃** affording the target molecular dyad **BDT-C₆₀**. Moreover, it is important to mention that the copper catalyzed reaction was selected over the thermal one to avoid any side reaction between the azido group and the C₆₀ itself by thermal decomposition into nitrenes [31–33].

Soluble in chloroform, the dyad was then characterized by UV-visible spectroscopy in both diluted solution (10^{−6} M) and as a thin film deposited by spin coating on glass (Figure 3). Optical data are presented in Table 1.

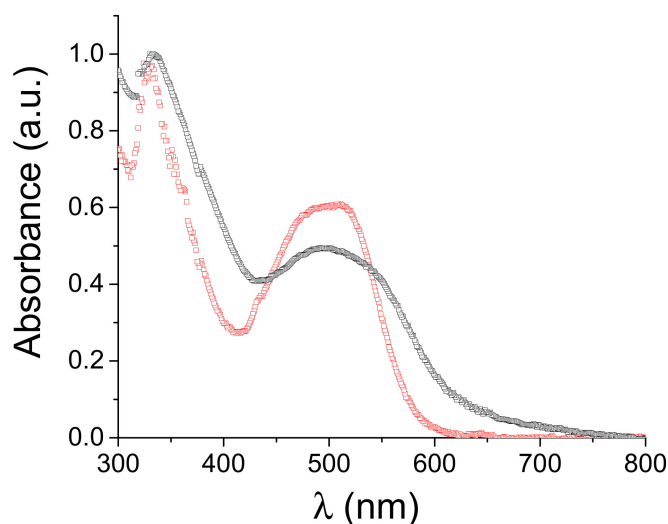


Figure 3. Normalized UV-Vis absorption spectra of **BDT-C₆₀** in chloroform solution (red) and as thin film on glass (black).

Spectra are characterized by two intense absorption bands with maxima (λ_{max}) at *ca* 330 nm and 520 nm assigned to the contribution of the fullerene and to an internal charge transfer (ICT) within the donor moiety, i.e., from the hydrazone moiety to the electron-deficient cyano vinyl ester respectively. Compared to the solution, the absorption spectra of the thin film broadens, leading to a red-shift of

the absorption edge and therefore a reduction of the optical energy gap (E_g^{opt}), thus estimated at *ca* 1.95 eV for the push-pull part.

Table 1. Optical and electrochemical data of **BDT-C₆₀**. UV-visible spectra recorded in a) chloroform and b) on glass; c) cyclic voltammetry performed on a 0.5 mM solution of **BDT-C₆₀** in 0.1 M Bu_4NPF_6 /dichloromethane, scan rate 100 mV s^{-1} , Pt working and counter electrodes, ref. Fc^+/Fc .

λ_{max} Solution (nm) ^a	ϵ ($L \cdot mol^{-1} \cdot cm^{-1}$) ^a	λ_{max} Thin Films (nm) ^b	λ_{onset} Thin Films (nm) ^b	ΔE_{opt} (eV) ^c	E_{pa}^1 (V) ^c	E_{pa}^2 (V) ^c	E_{pc}^1 (V) ^c	E_{pc}^2 (V) ^c	E_{pc}^3 (V) ^c	E_{pc}^4 (V) ^c
511	43800	500	635	1.95	0.64	0.90	-1.13	-1.46	-1.62	-2.01
330	71950	335								

In parallel, the cyclic voltammetry of the dyad was performed under inert atmosphere in dichloromethane using the tetrabutylammonium hexafluorophosphate (Bu_4NPF_6) as a supporting electrolyte and compared to that of the commercially available [6,6]-phenyl- C_{60} -butyric acid methyl ester (**PC₆₁BM**) (Figure 4).

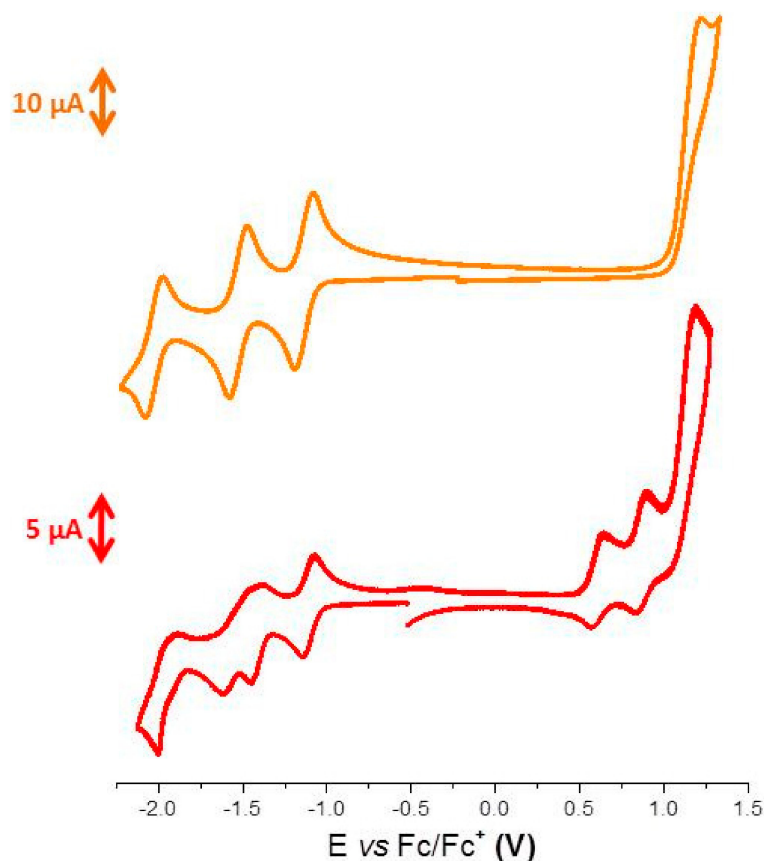


Figure 4. Cyclic voltammograms of **PC₆₁BM** (orange) and **BDT-C₆₀** (red).

Hence, in the negative region, four successive one-electron reduction waves are observed at $E_{pc} = -1.13\text{ V}$, -1.46 V , -1.62 V and -2.01 V respectively. In agreement with the electrochemical signature of the **PC₆₁BM**, the first, third and fourth reversible processes are associated to the step-by-step one-electron reduction of the fullerene moiety while the second irreversible wave can be assigned to the formation of the radical-anion localized on the push-pull system. In the anodic region, the latter exhibits two reversible oxidation waves at $E_{pa} = 0.64$ and 0.90 V attributed to the generation of a stable radical cation and dication respectively.

Once characterized at the molecular level, the **BDT-C₆₀** dyad was involved in the fabrication of organic solar cells to evaluate its potential as single-material. The active layer was thus

spun cast on indium tin oxide (ITO) patterned glass substrates pre-coated with a 40 nm layer of poly(3,4-ethylenedioxythiophene) polystyrene sulfonate (PEDOT-PSS). The quality of the films was examined by optical microscopy and atomic force microscopy (AFM) revealing, in the latter case, smooth and homogeneous surface topographies with a root mean square of *ca* 0.4 nm (Figure 5).

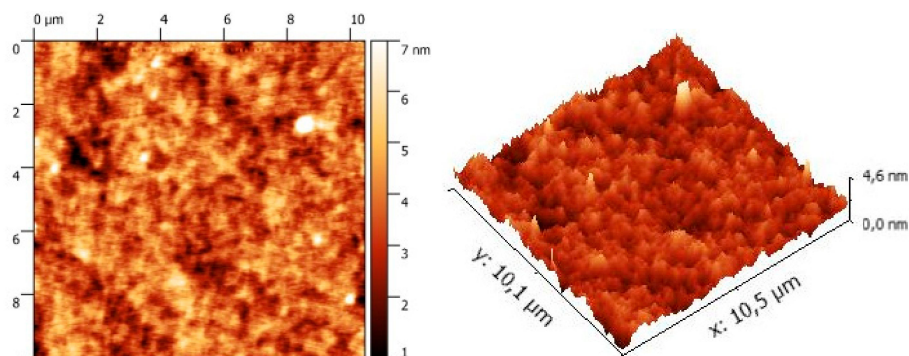


Figure 5. Atomic force microscopy (AFM) images of **BDT-C₆₀** based active layer ($10 \times 10 \mu\text{m}^2$).

Devices were achieved by evaporating 100 nm of aluminum through a shadow mask defining six cells of 27 mm^2 each. The best devices were obtained with film spun-cast at 4000 rpm from a chloroform solution containing $15 \text{ mg}\cdot\text{mL}^{-1}$ of the dyad. Hence, in these conditions, and despite a good open circuit voltage (V_{oc}) of *ca* 0.9 V, a modest maximum power conversion efficiency (PCE) of *ca* 0.5% was barely reached resulting from a low fill factor (FF) and short circuit current (J_{sc}) of 28% and $1.89 \text{ mA}\cdot\text{cm}^{-2}$, respectively (Figure 6).

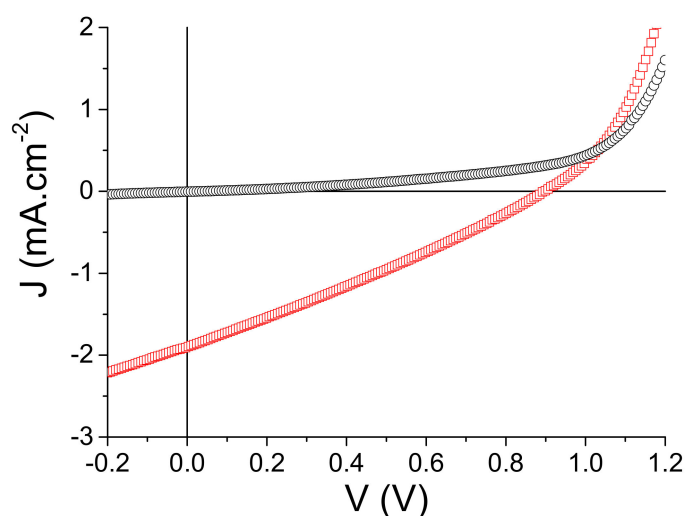


Figure 6. J–V characteristics of the **BDT-C₆₀** based single component organic solar cell in the dark (black circles) and under an AM. 1.5 simulated solar illumination at $100 \text{ mW}\cdot\text{cm}^{-2}$.

In parallel, external quantum efficiency (EQE) measurements were recorded on the best performing organic solar cells revealing an increased contribution of the fullerene derivative with regards to the push-pull moiety (Figure 7).

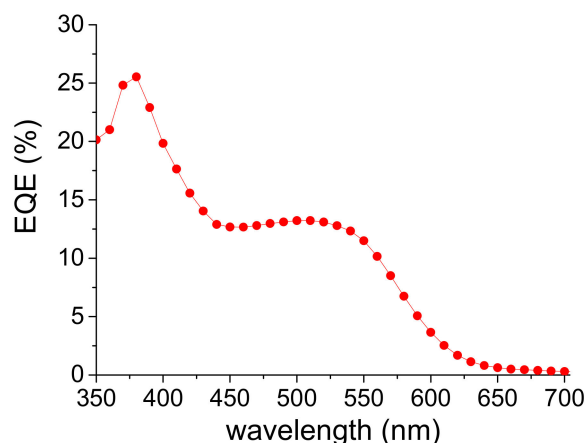


Figure 7. External quantum efficiency (EQE) curve of BDT-C₆₀ based device (integrated current density $J_{\text{int}} = 1.71 \text{ mA}\cdot\text{cm}^{-2}$).

In agreement with the UV-Visible experiments, the spectrum recorded under monochromatic irradiation shows an improved photon to electron conversion reaching 26% at 380 nm assigned to the contribution of the grafted fullerene vs. only 13% at 510 nm, correlated to the ICT band of the donor.

To gain further insights into these differences, hole-mobility (μ^h) of the dyad was assessed using the space-charge limited current (SCLC) method on hole-only devices of architecture ITO/PEDOT:PSS/BDT-C₆₀/gold (Figure 8) [23,34,35].

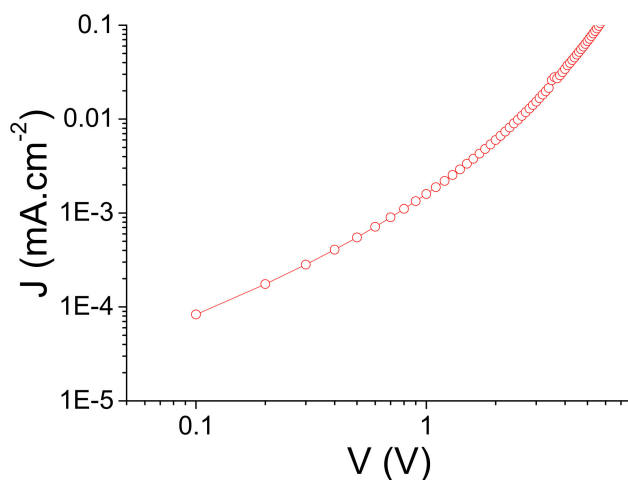


Figure 8. J-V characteristics of hole only devices ITO/PEDOT:PSS/BDT-C₆₀/Au.

It turns out that a significantly low value of $ca 4 \times 10^{-6} \text{ cm}^2\cdot\text{V}^{-1}\cdot\text{s}^{-1}$ was determined, thus contributing to the low FF and J_{sc} as well as difference of contribution recorded on the EQE spectrum between the two constituting units, namely the push-pull and the fullerene.

4. Conclusions

A new benzodithiophene (BDT) based push-pull was prepared, clicked to a fullerene derivative and evaluated as a single material for organic photovoltaic purposes. Although modest power conversion efficiencies were reached ($ca 0.5\%$) in such simple devices, they are at least up and running. These results once again demonstrate the difficulty to prepare an efficient single molecular material but, while remaining optimistic, better results can be reasonably expected. To achieve this complicated goal, one may improve the charge transport properties within the active layer and reach a good balance between both the hole and electron mobility. In addition, controlling the morphology also linked to the

transport properties, by favoring the interconnectivity between the constituting building blocks of the same nature (D with D and A with A), thus inducing a nanoscale phase segregation clearly appears to be a key parameter for success.

Author Contributions: Synthesis and characterization of the molecular structures, A.L., T.L., C.D. and Y.J.; Device fabrication, A.L., A.H.H.; AFM measurements, S.D.-S.; supervision, J.R., P.B., C.C.; writing C.C.

Funding: This research was funded by the LUMOMAT RFI (Région Pays de la Loire) under the SCOP project.

Acknowledgments: The RFI LUMOMAT from the Région Pays de la Loire and the Ministère de la Recherche are acknowledged for the PhD grants of A. Labrunie and C. Dalinot respectively. The University of Isfahan is thanked for the PhD grant of A. Habibi. The authors thank the MATRIX SFR of the University of Angers and more precisely the ASTRAL and CARMA platforms for the characterization of organic compounds and device preparation/characterization respectively.

Conflicts of Interest: The authors declare no conflict of interest.

References

1. Yuan, J.; Zhang, Y.; Zhou, L.; Zhang, G.; Yip, H.-L.; Lau, T.-K.; Lu, X.; Zhu, C.; Peng, H.; Johnson, P.A.; et al. Single-Junction Organic Solar Cell with over 15% Efficiency Using Fused-Ring Acceptor with Electron-Deficient Core. *Joule* **2019**, *3*, 1140–1151. [[CrossRef](#)]
2. Marszalek, T.; Li, M.; Pisula, W. Design directed self-assembly of donor–acceptor polymers. *Chem. Commun.* **2016**, *52*, 10938–10947. [[CrossRef](#)] [[PubMed](#)]
3. Duan, C.; Willems, R.E.M.; van Franeker, J.J.; Bruijnaers, B.J.; Wienk, M.M.; Janssen, R.A.J. Effect of side chain length on the charge transport, morphology, and photovoltaic performance of conjugated polymers in bulk heterojunction solar cells. *J. Mater. Chem. A* **2016**, *4*, 1855–1866. [[CrossRef](#)]
4. Liang, Y.; Feng, D.; Wu, Y.; Tsai, S.-T.; Li, G.; Ray, C.; Yu, L. Highly Efficient Solar Cell Polymers Developed via Fine-Tuning of Structural and Electronic Properties. *J. Am. Chem. Soc.* **2009**, *131*, 7792–7799. [[CrossRef](#)] [[PubMed](#)]
5. Beaujuge, P.M.; Fréchet, J.M.J. Molecular Design and Ordering Effects in π -Functional Materials for Transistor and Solar Cell Applications. *J. Am. Chem. Soc.* **2011**, *133*, 20009–20029. [[CrossRef](#)]
6. Labrunie, A.; Josse, P.; Dabos-Seignon, S.; Blanchard, P.; Cabanetos, C. Pentaerythritol based push–pull tetramers for organic photovoltaics. *Sustain. Energy Fuels* **2017**, *1*, 1921–1927.
7. Josse, P.; Dayneko, S.; Zhang, Y.; Dabos-Seignon, S.; Zhang, S.; Blanchard, P.; Welch, G.C.; Cabanetos, C. Direct (Hetero)Arylation Polymerization of a Spirobifluorene and a Dithienyl-Diketopyrrolopyrrole Derivative: New Donor Polymers for Organic Solar Cells. *Molecules* **2018**, *23*, 962. [[CrossRef](#)] [[PubMed](#)]
8. Josse, P.; Favereau, L.; Shen, C.; Dabos-Seignon, S.; Blanchard, P.; Cabanetos, C.; Crassous, J. Enantiopure versus Racemic Naphthalimide End-Capped Helicenic Non-fullerene Electron Acceptors: Impact on Organic Photovoltaics Performance. *Chem. Eur. J.* **2017**, *23*, 6277–6281. [[CrossRef](#)]
9. Swinnen, A.; Haeldermans, I.; vande Ven, M.; D’Haen, J.; Vanhoyland, G.; Aresu, S.; D’Olieslaeger, M.; Manca, J. Tuning the Dimensions of C60-Based Needlelike Crystals in Blended Thin Films. *Adv. Funct. Mater.* **2006**, *16*, 760–765. [[CrossRef](#)]
10. Dang, M.T.; Hirsch, L.; Wantz, G. P3HT: PCBM, Best Seller in Polymer Photovoltaic Research. *Adv. Mater.* **2011**, *23*, 3597–3602. [[CrossRef](#)]
11. Liao, H.-C.; Ho, C.-C.; Chang, C.-Y.; Jao, M.-H.; Darling, S.B.; Su, W.-F. Additives for morphology control in high-efficiency organic solar cells. *Mater. Today* **2013**, *16*, 326–336. [[CrossRef](#)]
12. Roncali, J.; Grosu, I. The Dawn of Single Material Organic Solar Cells. *Adv. Sci.* **2019**, *6*, 1801026. [[CrossRef](#)]
13. Roncali, J. Single Material Solar Cells: The Next Frontier for Organic Photovoltaics? *Adv. Energy Mater.* **2011**, *1*, 147–160. [[CrossRef](#)]
14. Segura, J.L.; Martín, N.; Guldi, D.M. Materials for organic solar cells: The C60/ π -conjugated oligomer approach. *Chem. Soc. Rev.* **2005**, *34*, 31–47. [[CrossRef](#)]
15. Chen, T.L.; Zhang, Y.; Smith, P.; Tamayo, A.; Liu, Y.; Ma, B. Diketopyrrolopyrrole-Containing Oligothiophene-Fullerene Triads and Their Use in Organic Solar Cells. *ACS Appl. Mater. Interfaces* **2011**, *3*, 2275–2280. [[CrossRef](#)] [[PubMed](#)]
16. Izawa, S.; Hashimoto, K.; Tajima, K. Efficient charge generation and collection in organic solar cells based on low band gap dyad molecules. *Chem. Commun.* **2011**, *47*, 6365–6367. [[CrossRef](#)] [[PubMed](#)]

17. Bu, L.; Guo, X.; Yu, B.; Qu, Y.; Xie, Z.; Yan, D.; Geng, Y.; Wang, F. Monodisperse Co-oligomer Approach toward Nanostructured Films with Alternating Donor–Acceptor Lamellae. *J. Am. Chem. Soc.* **2009**, *131*, 13242–13243. [[CrossRef](#)]
18. Bu, L.; Guo, X.; Yu, B.; Fu, Y.; Qu, Y.; Xie, Z.; Yan, D.; Geng, Y.; Wang, F. Donor–acceptor liquid crystalline conjugated cooligomers for the preparation of films with the ideal morphology for bulk heterojunction solar cells. *Polymer* **2011**, *52*, 4253–4260. [[CrossRef](#)]
19. Qu, J.; Gao, B.; Tian, H.; Zhang, X.; Wang, Y.; Xie, Z.; Wang, H.; Geng, Y.; Wang, F. Donor–spacer–acceptor monodisperse conjugated co-oligomers for efficient single-molecule photovoltaic cells based on non-fullerene acceptors. *J. Mater. Chem. A* **2014**, *2*, 3632–3640. [[CrossRef](#)]
20. Labrunie, A.; Londi, G.; Dayneko, S.V.; Blais, M.; Dabos-Seignon, S.; Welch, G.C.; Beljonne, D.; Blanchard, P.; Cabanetos, C. A triazatruxene-based molecular dyad for single-component organic solar cells. *Chem. Squared* **2018**, *2*, 3. [[CrossRef](#)]
21. Nguyen, T.L.; Lee, T.H.; Gautam, B.; Park, S.Y.; Gundogdu, K.; Kim, J.Y.; Woo, H.Y. Single Component Organic Solar Cells Based on Oligothiophene-Fullerene Conjugate. *Adv. Funct. Mater.* **2017**, *27*, 1702474. [[CrossRef](#)]
22. Narayanaswamy, K.; Venkateswararao, A.; Nagarjuna, P.; Bishnoi, S.; Gupta, V.; Chand, S.; Singh, S.P. An Organic Dyad Composed of Diathiafulvalene-Functionalized Diketopyrrolopyrrole–Fullerene for Single-Component High-Efficiency Organic Solar Cells. *Angew. Chem. Int. Ed.* **2016**, *55*, 12334–12337. [[CrossRef](#)] [[PubMed](#)]
23. Labrunie, A.; Gorenflot, J.; Babics, M.; Alévêque, O.; Dabos-Seignon, S.; Balawi, A.H.; Kan, Z.; Wohlfahrt, M.; Levillain, E.; Hudhomme, P.; et al. Triphenylamine-Based Push–Pull σ -C60 Dyad As Photoactive Molecular Material for Single-Component Organic Solar Cells: Synthesis, Characterizations, and Photophysical Properties. *Chem. Mater.* **2018**, *30*, 3474–3485. [[CrossRef](#)]
24. Warnan, J.; Cabanetos, C.; Bude, R.; El Labban, A.; Li, L.; Beaujuge, P.M. Electron-Deficient N-Alkylolyl Derivatives of Thieno[3,4-c]pyrrole-4,6-dione Yield Efficient Polymer Solar Cells with Open-Circuit Voltages > 1 V. *Chem. Mater.* **2014**, *26*, 2829–2835. [[CrossRef](#)]
25. Warnan, J.; El Labban, A.; Cabanetos, C.; Hoke, E.T.; Shukla, P.K.; Risko, C.; Brédas, J.-L.; McGehee, M.D.; Beaujuge, P.M. Ring Substituents Mediate the Morphology of PBDTTPD-PCBM Bulk-Heterojunction Solar Cells. *Chem. Mater.* **2014**, *26*, 2299–2306. [[CrossRef](#)]
26. Cabanetos, C.; El Labban, A.; Bartelt, J.A.; Douglas, J.D.; Mateker, W.R.; Fréchet, J.M.J.; McGehee, M.D.; Beaujuge, P.M. Linear Side Chains in Benzo[1,2-b:4,5-b']dithiophene–Thieno[3,4-c]pyrrole-4,6-dione Polymers Direct Self-Assembly and Solar Cell Performance. *J. Am. Chem. Soc.* **2013**, *135*, 4656–4659. [[CrossRef](#)] [[PubMed](#)]
27. Graham, K.R.; Cabanetos, C.; Jahnke, J.P.; Idso, M.N.; El Labban, A.; Ngongang Ndjawa, G.O.; Heumueller, T.; Vandewal, K.; Salleo, A.; Chmelka, B.F.; et al. Importance of the Donor:Fullerene Intermolecular Arrangement for High-Efficiency Organic Photovoltaics. *J. Am. Chem. Soc.* **2014**, *136*, 9608–9618. [[CrossRef](#)] [[PubMed](#)]
28. Jiang, Y.; Cabanetos, C.; Allain, M.; Liu, P.; Roncali, J. Molecular electron-acceptors based on benzodithiophene for organic photovoltaics. *Tetrahedron Lett.* **2015**, *56*, 2324–2328. [[CrossRef](#)]
29. Wang, Z.B.; Helander, M.G.; Greiner, M.T.; Qiu, J.; Lu, Z.H. Carrier mobility of organic semiconductors based on current-voltage characteristics. *J. Appl. Phys.* **2010**, *107*, 034506. [[CrossRef](#)]
30. Diac, A.; Demeter, D.; Allain, M.; Grosu, I.; Roncali, J. Simple and Versatile Molecular Donors for Organic Photovoltaics Prepared by Metal-Free Synthesis. *Chem. Eur. J.* **2015**, *21*, 1598–1608. [[CrossRef](#)]
31. Huisgen, R.; Blaschke, H. 1.3-Dipolare Cycloadditionen, XX: 2-Äthoxy-oxazole aus Äthoxycarbonyl-azen und Alkinen. *Chem. Ber.* **1965**, *98*, 2985–2997. [[CrossRef](#)]
32. Huisgen, R. 1,3-Dipolar Cycloadditions. Past and Future. *Angew. Chem. Int. Ed.* **1963**, *2*, 565–598. [[CrossRef](#)]
33. Kahle, F.-J.; Saller, C.; Köhler, A.; Strohriegel, P. Crosslinked Semiconductor Polymers for Photovoltaic Applications. *Adv. Energy Mater.* **2017**, *7*, 1700306. [[CrossRef](#)]
34. Labrunie, A.; Jiang, Y.; Baert, F.; Leliège, A.; Roncali, J.; Cabanetos, C.; Blanchard, P. Small molecular push–pull donors for organic photovoltaics: Effect of the heterocyclic π -spacer. *RSC Adv.* **2015**, *5*, 102550–102554. [[CrossRef](#)]
35. Jiang, Y.; Allain, M.; Gindre, D.; Dabos-Seignon, S.; Blanchard, P.; Cabanetos, C.; Roncali, J. Thermally induced crystallization, hole-transport, NLO and photovoltaic activity of a bis-diarylamine-based push-pull molecule. *Sci. Rep.* **2017**, *7*, 8317. [[CrossRef](#)] [[PubMed](#)]

